Communications

Small UWB Planar Monopole Antenna With Added GPS/GSM/WLAN Bands

Ali Foudazi, Hamid Reza Hassani, and Sajad Mohammad ali nezhad

***Abstract*—A small-size microstrip-fed multi-band planar monopole antenna is presented. The base of the proposed antenna is a diamond-shaped-patch (DSP) that covers the ultrawideband (UWB) frequency range. To create a multi-band antenna, several narrow strips, acting as resonance paths, can be integrated with the DSP antenna. It is shown that by removing the centre part of the DSP antenna, without distorting the UWB behavior, quarter-wavelength strips can be added to the notched region. This will not affect the dimension of the base antenna. The designed quad-band antenna has a substrate size of 16×22 mm^2 and covers the frequency bands 1.3, 1.8, 2.4 and 3.1–10.6 GHz which includes GPS, GSM, WLAN and UWB. Dual-, triple- and quad-band antennas are simulated and good results are obtained. The antennas have omnidirectional and stable radiation patterns across all the relevant bands. Moreover, relatively consistent group delays across the UWB frequencies are noticed for the base, dual- and triple-band antennas, and slightly distorted for the quad-band antenna. A prototype of the quad-band antenna is fabricated and measured results are compared with simulated results.**

***Index Terms*—Monopole antenna, multi-band antenna, ultrawideband (UWB) antenna, wireless communication frequencies.**

I. Introduction

The ultrawideband (UWB) communication systems have received great attention from both the academic and the industrial sectors as a result of commercial systems such as indoor and hand-held wireless communication. UWB is a short distance radio communication technology that can perform high-speed communication with speeds of more than 100 Mbps. The UWB systems can be divided into two categories: direct sequence UWB (DS-UWB) and multi-band orthogonal frequency division multiplexing (MB-OFDM). The DS-UWB proposal foresees two different carrier frequencies at 4.104 (low band: 3.1–5.15 GHz) and 8.208 GHz (high band: 5.825–10.6 GHz), while the MB-OFDM format in IEEE 802.15.3 a has an interval between 3.1 and 10.6 GHz and is divided into 14 subintervals. Each subinterval covers 528 MHz of bandwidth [1], [2].

Modern communication systems require a single antenna to cover several allocated wireless frequency bands. Moreover, design of a multi-band antenna which also covers the UWB range without deteriorating the UWB performance is of high interest. Also, a significant issue in communication systems is to miniaturize the antenna while providing good performance over the bands. Planar printed monopole antennas, due to their attractive features such as low cost, simple structure, ease of fabrication, wide bandwidth, and omnidirectional radiation pattern have received great attention for UWB systems [3]–[9].

There are two techniques reported in the literature to create multi-band printed monopole antennas. In the first, a patch antenna is designed to cover the desired wide bandwidth. The lower limit of the frequency band increases the size of the antenna to be large. To create the multi-band behavior, notches are then introduced into the antenna [10], [11]. In the second technique, a small-size antenna can be designed to cover the highest frequency band, and by adding extra resonant elements to the main body, lower frequency bands can be created [12], [13]. In [12], by using a triangular-shaped patch and a pair of additional arms at the two corners of the patch, a dual-band antenna is created. In [13], at the corner of a UWB monopole antenna, an L-shaped resonant element is added to integrate the Bluetooth band with the existing UWB. The overall size of the antenna is 42×46 mm^2. Based on the literature review, it would seem that in the second technique, there is no antenna structure in which for a given substrate more than two bands can be created.

In this communication, the second technique mentioned above is used. A base diamond-shaped-patch (DSP) antenna is considered to cover the UWB range. By inserting a notched region in the middle part of the DSP antenna and adding quarter-wavelength strips, a multi-band antenna is achieved. The novelty of the present method is that the resonant strips can be added to the base structure without affecting the UWB behavior. The size of the proposed multi-band antenna substrate is kept the same as the base antenna. Simulated results of dual-, triple- and quad-band antennas are presented along with the measured results of the quad-band antenna. The simulation is carried out via HFSS software package.

II. UWB Antenna Design

The structure of a suitable planar monopole radiator can be used as the base for the eventual multi-band antenna, operating over the UWB frequency range, is shown in Fig. 1(a). This base UWB antenna can be referred to as the DSP antenna. The antenna uses FR4 substrate with a dimension of $16 \times 22 \times 1$ mm^3, $\varepsilon_{\mathrm{r}} = 4.4$ and a loss tangent of 0.02. The width (W_f) of the microstrip-fed line is fixed at 1.86 mm to achieve 50 Ω characteristic impedance, and is connected to the DSP via a line of length L_f. A simple rectangular conducting ground plane of width W_s and length L_g is placed on the other side of the substrate.

In designing the multi-band antenna, the DSP antenna is considered to cover the UWB range, which is the highest frequency band of the antenna. As shown in Fig. 1(a), there are four parameters $a1$, $a2$, $b1$, and $b2$ that could affect the performance of the UWB antenna. To obtain a small-size antenna that covers the UWB range, parametric studies for these four parameters are carried out and results of reflection coefficient are presented. From Fig. 2(a), it is clear that the DSP antenna of Fig. 1(a) should be beveled along the lower side (near the ground plane) to improve the reflection coefficient characteristic over the desired band $(b1)$. Furthermore, for a constant $b1$, the value of $b2$ changes the lower cut-off frequency of the DSP antenna. Also, as shown in Fig. 2(b), an appropriate value of $a1$ can improve the reflection coefficient at higher frequencies and provide wider impedance matching over the UWB range.

It can be shown that the current distribution over this DSP antenna is mostly concentrated over the outside edges of the patch with negligible current in the centre region [14]. Thus, a rectangular section along the

Manuscript received July 24, 2010; revised November 08, 2011; accepted November 11, 2011. Date of publication May 03, 2012; date of current version May 29, 2012

The authors are with the Electrical and Electronic Engineering Department, Shahed University, Tehran, Iran (e-mail: foudazi@shahed.ac.ir; alinezhad@shahed.ac.ir; hassani@shahed.ac.ir).

Color versions of one or more of the figures in this communication are available online at http://ieeexplore.ieee.org.

Digital Object Identifier 10.1109/TAP.2012.2194632

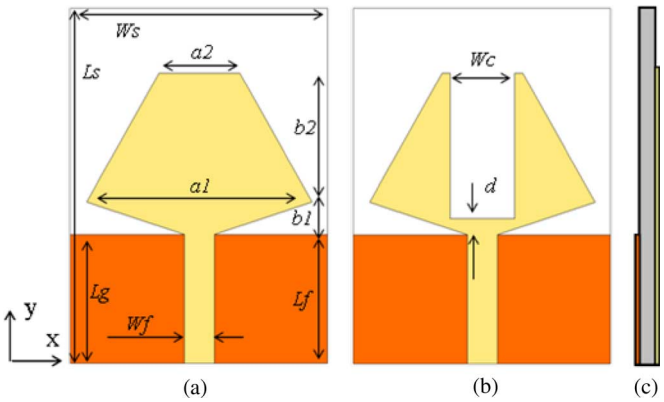

Fig. 1. (a) DSP UWB antenna, (b) DSP antenna with inserting notched region in the middle part, (c) side view of the proposed base antenna.

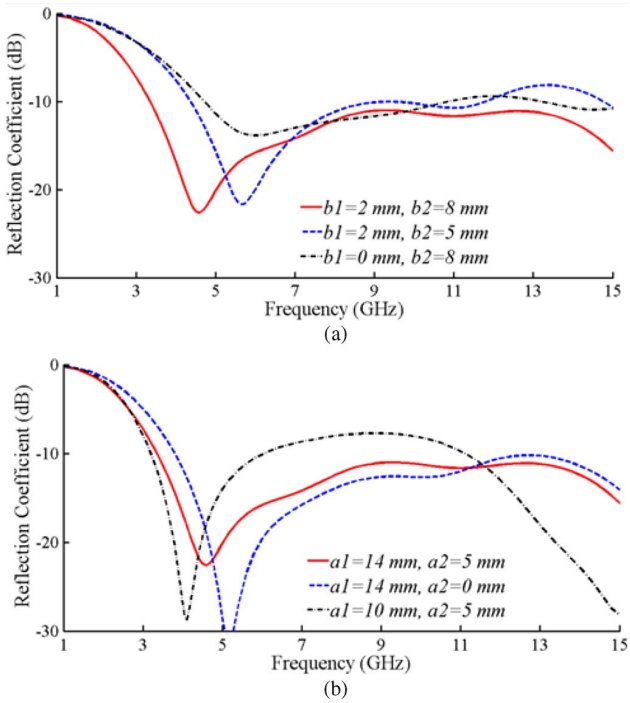

Fig. 2. Simulated reflection coefficient of the simple DSP antenna (without the notched region) for (a) $a1 = 14$ mm, $a2 = 5$ mm with various $b1$ and $b2$ and for (b) $b1 = 2$ mm, $b2 = 8$ mm with various $a1$ and $a2$.

axis of the DSP antenna can be removed as shown in Fig. 1(b), without affecting the overall antenna impedance and radiation characteristics leading to the UWB antenna [15]. This adjustment also ensures a symmetrical design of the antenna. Results of Fig. 2(b) show that parameter $a2$ does not have a significant effect on the reflection coefficient. But it should be large enough so that when a rectangular section is removed, as shown in Fig. 1(b), several resonant strips can be placed within the notched region to design a multi-band antenna. Fig. 3 shows the reflection coefficient of the DSP antenna with and without the notched region. It is seen that narrow notched region has almost no effect on the reflection coefficient results. Also, increasing Wc has no effect on cut-off frequency of the base patch.

III. Multi-Band Antenna Design

It is desired to have other frequency bands at specific wireless communication frequencies below the UWB. In this section, the *centre feed*

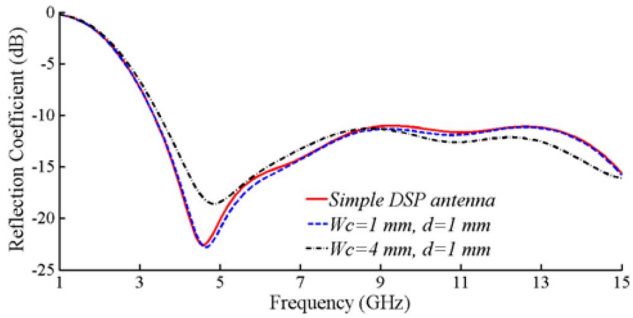

Fig. 3. Simulated reflection coefficient of the DSP antenna before and after inserting notched region for various width of the cut out section Wc. ($a1 = 14$ mm, a2 $= 5$ mm, $b1 = 2$ mm, $b2 = 8$ mm, $L_f = 8$ mm, $L_g = 8$ mm).

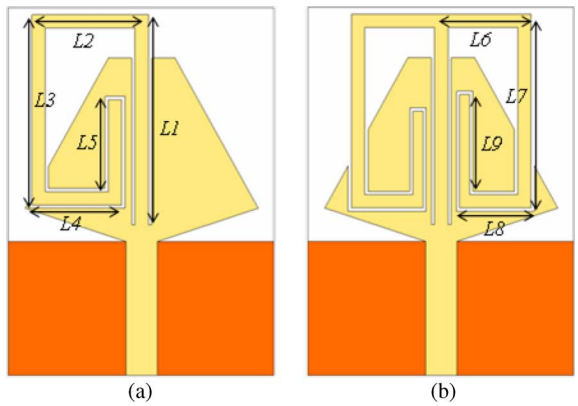

Fig. 4. Multi-band DSP antenna configurations for (a) dual-band, (b) triple-band applications.

method is introduced and used to design small-size dual-, triple- and quad-band antennas. In [3], a notched region is introduced in a UWB radiator, resulting in reduce the effect of ground plane and RF cabling loss at lower frequencies. After the creation of the notched region, the resonance length of the created path is $\lambda/2$.

As shown in the previous section, one can insert a notched region into the base patch antenna without affecting the characteristics of the antenna. To obtain multi-band behavior, additional resonant strips can be placed in the notched region. These strips are efficiently excited, if placed along the direction of the current flow and near the main microstrip feed line, i.e. at position $L_f + d$. This technique of creating a multi-band antenna can be referred to as the *centre feed method*. Fig. 4(a) shows a dual-band antenna structure using this centre feed method. For a desired resonant frequency the wavelength is given by

$$\lambda_g = \frac{\lambda}{\sqrt{\varepsilon_{reff}}} \tag{1}$$

which λ is the free space wavelength and ε_{reff} is effective permittivity which is given by the approximate formula of

$$\varepsilon_{reff} \approx \frac{\varepsilon_r + 1}{2}. \tag{2}$$

The exact equation of effective permittivity includes substrate thickness. For low thicknesses it can be shown that effective permittivity is mostly dependent on the terms given in (2) [3], [8]. The total required

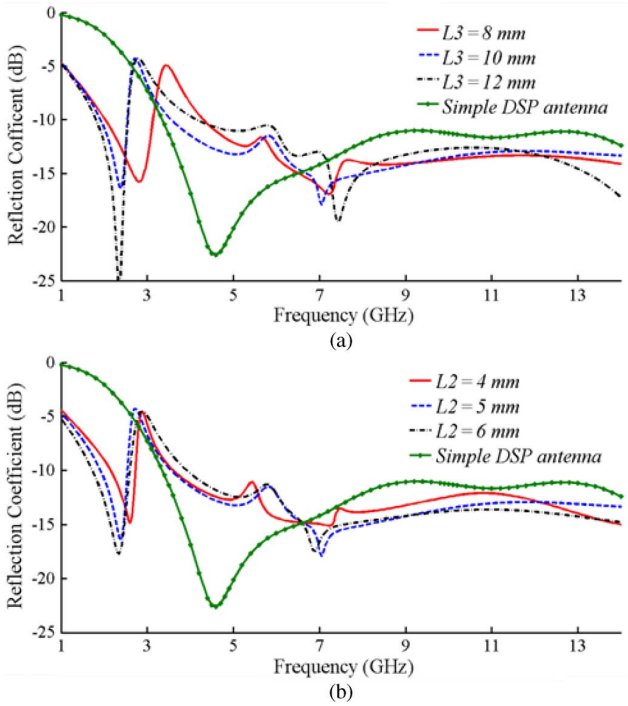

Fig. 5. Reflection coefficient of the dual-band WLAN/UWB antenna with (a) $L2 = 5$ mm for various values of $L3$, (b) $L3 = 10$ mm for various values of $L2$, with removed $L4$ and $L5$. ($a1 = 14$ mm, $a2 = 4$ mm, $b1 = 2$ mm, $b2 = 9$ mm, $L1 = 12$ mm, $Wc = 1.4$ mm, $d = 1$ mm, and other parameters similar to those of Fig. 3)

TABLE I
STRIP LENGTHS FOR VARIOUS RESONANT FREQUENCIES WITH UWB BAND

Frequency (GHz)	Arm Length (mm)				
	L1	*L2*	*L3*	*L4*	*L5*
1.3	12.6	6.2	9.8	5.4	5.5
1.8	12.6	6.1	9.8	5.4	removed
2.4	12.6	5	10	removed	removed

resonant strip length, which is a multiple of quarter-wavelength, can be calculated approximately by [16]

$$L_{total} \approx n\frac{\lambda_g}{4}. \tag{3}$$

By using the *centre feed method*, a segment of the added strips can be placed within the notched region of the base patch while the remaining sections are brought back towards the patch. Even though strips are added to the base antenna, the overall substrate dimension has not changed, leading to small-size multi-band antenna.

A. Dual- and Triple-Band Antenna Configuration

In this section, the design of a dual- and triple-band antenna is presented. The structures of the proposed antennas are shown in Fig. 4. In all these structures, the width of the slot lines, between the added strips and the base patch, is set at 0.2 mm and has negligible effect on the antenna performance.

Fig. 5 shows the reflection coefficient of a dual-band antenna with single strip when either length $L2$ or $L3$ is fixed while the other length is varied. From Fig. 5(a), it is seen that the increase in $L3$ decreases the resonant frequency of the band, while Fig. 5(b) shows that the increase in $L2$ decreases the resonant frequency and disturbs the impedance matching slightly. The results shown in Fig. 5 are suitable

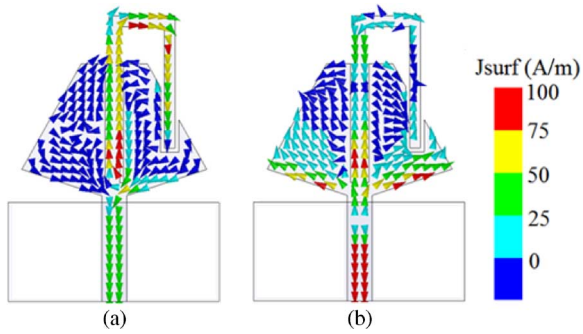

Fig. 6. Current distribution on the dual-band WLAN/UWB antenna at (a) 2.4 GHz and (b) 6 GHz.

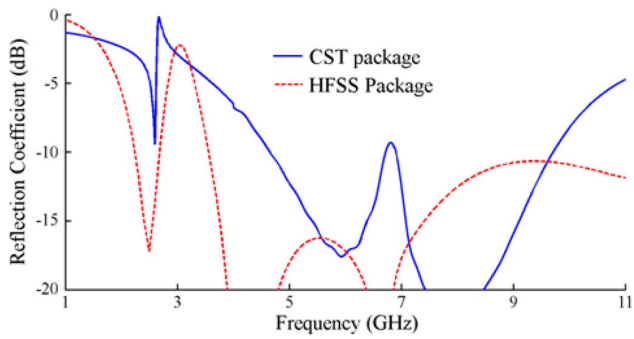

Fig. 7. Simulated reflection coefficient of the dual-band WLAN/UWB antenna as obtained by two different commercial software packages.

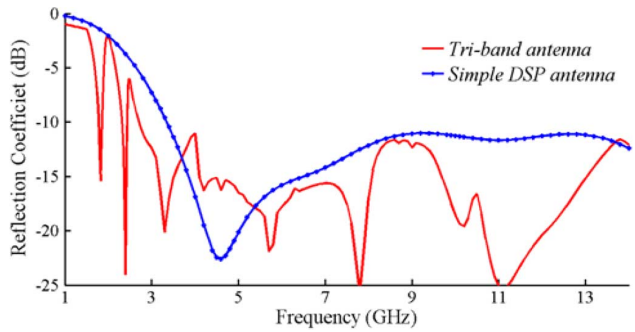

Fig. 8. Reflection coefficient of the tri-band GSM/WLAN/UWB antenna for $L1 = 12.6$ mm, $L2 = 6.2$ mm, $L3 = 10$ mm, $L4 = 1$ mm, $L6 = 6.2$ mm, $L7 = 9.8$ mm, $L8 = 5.4$ mm, and $L5$ and $L9$ removed.

for WLAN/UWB applications. To obtain any resonant frequencies between 1.3 GHz and 2.4 GHz (i.e. to integrate GPS, GSM or WLAN with UWB antenna) for the dual-band structure, the required length of the strips should be set according to Table I for the lower frequency band. Also, the dimension of the DSP antenna is kept fixed for the UWB range.

The simulated current distribution of the dual-band antenna structure of Fig. 4(a) for WLAN/UWB configuration at 2.4 and 6 GHz are presented in Fig. 6. As shown in Fig. 6(a), the base patch of the dual-band antenna at 2.4 GHz has negligible current, while on the added strip maximum current is seen at the beginning and minimum current at the end of the strip which, according to (3), confirms that the length of the strip is about quarter-wavelength. Fig. 6(b) shows that at a frequency of 6 GHz the base patch has appreciable current while the current on the added strip runs in opposite directions leading to negligible effect on radiation. It means that the added strips and the main body of the

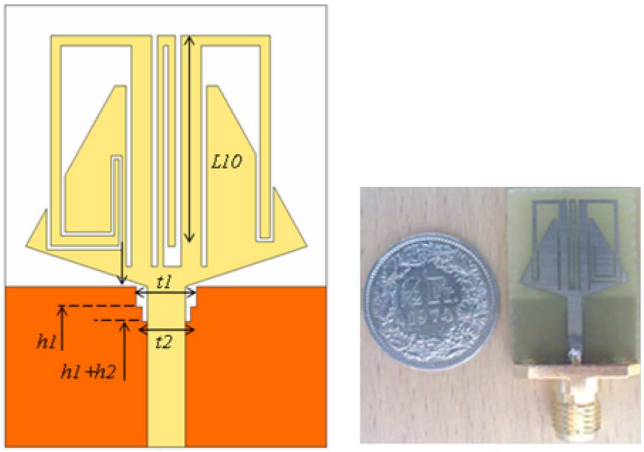

Fig. 9. (a) The structure of the Quad-band antenna with steps on the ground with $t1 = 3$ mm, $t2 = 2.4$ mm, $h1 + h2 = 1.75$ mm and (b) the structure of the fabricated antenna.

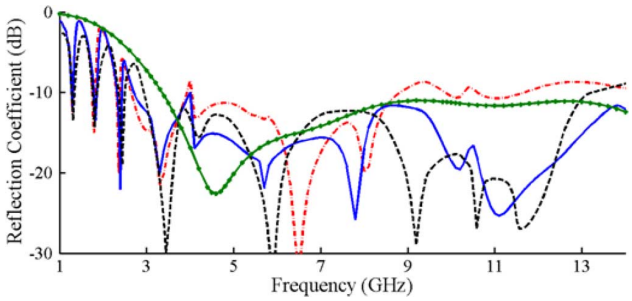

Fig. 10. Simulated and measured reflection coefficient of the quad-band antenna ((—•—) simulated simple DSP antenna, -·- simulated Quad-band without step, — simulated Quad-band with two steps, – – – measured Quad-band with two steps).

antenna do not have much effect on each other. As the operation frequency of the antenna increases, the guided wavelength of the structure (λ_g) decreases, resulting in the feed line length being several times that of the wavelengths.

It is known that different software packages can provide different results for a given antenna design [17]. As such, the above designed antenna as obtained by HFSS has also been simulated through a second software package, CST. The results show that the dimension of the added strips lead to similar behavior by using both HFSS and CST packages, while the dimension of the base patch antenna needs to be slightly tuned when using CST in order to provide similar behavior within the UWB range as that of HFSS. In Fig. 7, the differences between the results of the two packages can be seen.

Fig. 8 presents the reflection coefficient of a triple-band antenna shown in Fig. 4(b). The dimensions of the two strips are considered to have triple-band GSM/WLAN/UWB antenna. It is seen that the triple-band antenna has good resonances at 1.8 and 2.4 GHz and also suitable reflection coefficient below -10 dB over the UWB range.

B. Quad-Band Antenna Configuration

To create a quad-band antenna, apart from the base UWB antenna, three additional strips should be added to the structure in order to create the extra three bands below the UWB frequency. The proposed quad-band structure is shown in Fig. 9(a). Similar to the previous section, the centre part of the DSP is notched and two strips are added resulting in

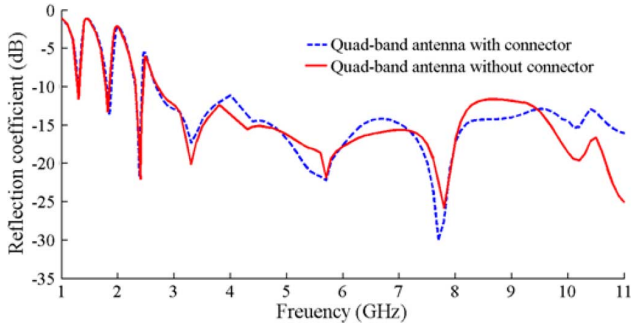

Fig. 11. Simulated reflection coefficient of the quad-band antenna with two steps, with and without the effects of the connector on antenna performances

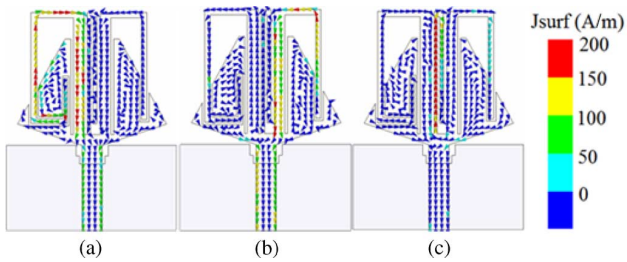

Fig. 12. Current distribution on the proposed quad-band antenna at (a) 1.3 GHz, (b) 1.8 GHz and (c) 2.4 GHz.

a triple-band behavior. To create the fourth band, a third strip is placed in between the other two strips. To keep the size of this strip compact within the given substrate size, this strip should also be brought back towards the base patch. If this is done either towards the left or right hand side of the existing strips, the resonance of the previous strips would be lost. Therefore, third strip is brought back towards itself on a path along the axis of the patch. Due to limitation of the length for this centre strip, it can only be used for resonances just below the UWB range, e.g., WLAN band at 2.4 GHz.

The three strips added to the base antenna structure would generate higher frequency harmonics that would affect the reflection coefficient as well as the impedance matching of the previous antennas. The performance of the antenna can be improved by placing steps in the ground plane around the feed line [18]. Fig. 10 shows the simulated reflection coefficient of the quad-band antenna with and without the steps as well as the measured reflection coefficient of the proposed quad-band antenna with two steps. As seen, four practical frequency bands, GPS (1.26–1.3), GSM (1.71–1.88), WLAN (2.4–2.48), and the UWB (3.1–10.6) GHz with good filtering effect between the bands is achieved. The fabricated proposed quad-band antenna is shown in 9(b). From the results shown in Fig. 10, it is noticed that the two steps in ground plane results in a better impedance matching over the UWB range. The overall dimension of the quad-band GPS/GSM/WLAN/UWB antenna is: $Wc = 4, L1 = 12.6, L2 = 5, L3 = 10.5, L4 = 3.5, L5 = 4.5, L6 = 4.5, L7 = 10, L10 = 10$ mm and $L8$ and $L9$ are removed.

Due to the small-size configuration of the antenna, the connector and cabling are comparable with the antenna size and can have an effect on the measured reflection coefficient. This could be a reason why there are differences between the simulated and measured results. It should be mentioned that in printed monopole antennas the ground plays the role of the other pole and thus, when the connector is attached to the feed line, it changes the current distribution on the ground plane. In fact, the connector adds up the current on its outer shell and this causes differences between simulation and measurement results for antenna

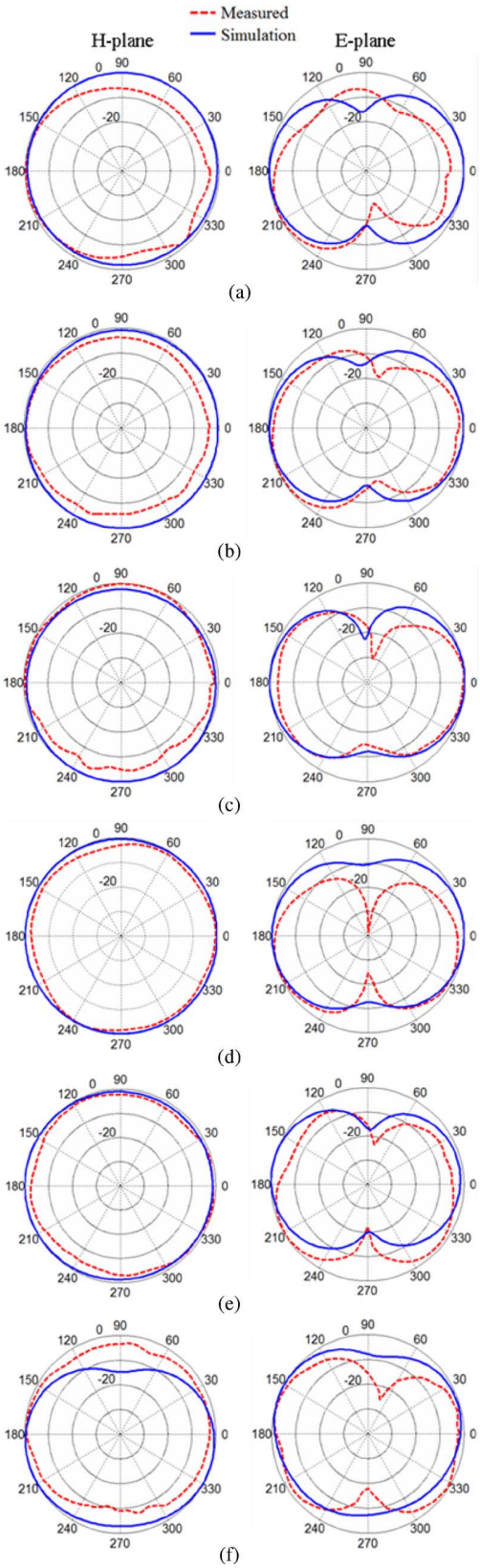

Fig. 13. E-(right column) and H-(left column) plane radiation pattern of the quad-band antenna at various frequencies of (a) 1.3, (b) 1.8, (c) 2.4, (d) 3, (e) 5, (f) 8 GHz.

behavior. In fact the connector shell plays part of the ground now and it causes a change in the current distribution on the pole of the antenna

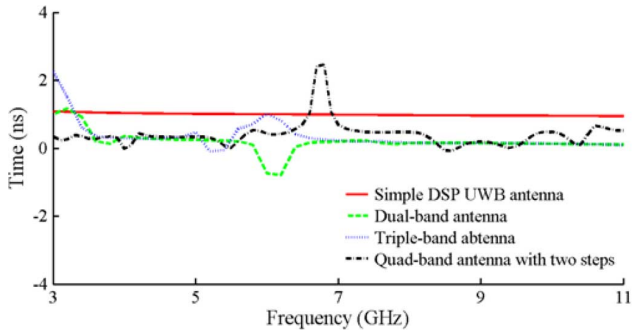

Fig. 14. The group delay of the proposed quad-band antenna for side-by-side configuration.

[5]. In Fig. 10, the differences between simulation and measurement results of the quad-band antenna are presented. The results presented in this communication are obtained by using a simple excitation wave port in HFSS. To confirm the validity of the simulated results when cabling and connector are included in the antenna, Fig. 11 presents the relevant comparison which shows slight differences at higher frequencies.

The current distribution on the proposed quad-band antenna at frequencies of 1.3, 1.8 and 2.4 GHz are shown in Fig. 12(a)–(c), respectively. At any of these frequencies the strip whose length is multiple of $\lambda_g/4$, according to (3), is clearly seen to be the resonant strip.

The radiation patterns of the base DSP, dual-, triple- and quad-band antennas are investigated. It is seen that the multi-band antennas provide omnidirectional radiation patterns in the H-plane (x-z plane) and stable patterns in the form of figure-eight in the E-plane (y-z plane). These results are similar to those of ordinary dipole antennas. Also, the measured and simulated E- and H-plane radiation patterns of the proposed quad-band antenna of Fig. 9 at the desired frequencies of 1.3, 1.8, 2.4, 3, 5 and 8 GHz are shown in Fig. 13. It is seen that the proposed antenna has stable radiation pattern characteristics over the quad-band frequencies. The measured results do include the cabling and connector effect which is more apparent at the lower frequencies, i.e. 1.3 GHz.

In order to verify the capability of the proposed antenna to operate as a UWB antenna, it is necessary to achieve a consistent group delay. The group delay properties of the proposed multi-band antenna have been studied and results shown in Fig. 14 can be summarized as below:

a) The base DSP antenna is first considered and results show that the group delay is flat with variations below 0.05 ns.
b) Addition of the first and second strips to the base antenna leads to dual- and triple-band antenna, showing that the group delay is flat with variations below 1 ns. As mentioned in [19], a group delay with variation up to 1 ns is acceptable.
c) It is noticed that when a third strip is added to the base structure, due to the large slot created within the main patch antenna, the group delay properties of the UWB antenna become distorted at 7 GHz leading to some 2.5 ns delay. From the results shown in Fig. 14, one can see that for the proposed antenna structure good UWB performance can be achieved with up to the triple-band application. The group delay result of the quad-band antenna structure shows that the antenna is not suitable for UWB applications. As mentioned before, the MB-OFDM divides the UWB range into 14 subintervals with 528 MHz bandwidth [2]. The proposed quad-band antenna can be used for this application.

IV. Conclusion

A diamond shaped microstrip patch antenna with included narrow strips leading to a small size multi-band planar monopole antenna has been presented. The diamond shaped patch antenna covers the UWB

frequency range. By changing the length of the added resonant strips in the notched region, the centre frequency of the multi resonances below the UWB frequency can be finely tuned. The fabricated antenna has been designed for frequency bands 1.3, 1.8, 2.4 and 3.1–10.6 GHz that covers the GPS, GSM, WLAN and the UWB, respectively. The dual and triple-band antennas show stable omnidirectional radiation patterns over all the frequency bands as well as relatively consistent group delay across the UWB frequencies. The proposed quad-band antenna is suitable for MB-OFDM applications.

ACKNOWLEDGMENT

The authors gratefully acknowledge Prof. G. A. Vandenbosch from Katholieke Universiteit Leuven for fruitful discussions. Special thanks to Dr. Mohammadpour-Aghdam from University of Tehran for his help in experimental parts.

REFERENCES

[1] Batra, "Multiband OFDM physical layer proposal for IEEE 802.15 task group 3a," *IEEE Document 802.15-04-0493r1*, 2003.

[2] R. Kohno, M. McLaughlin, and M. Welborn, "DS-UWB physical layer submission to 802.15 task group 3a," *IEEE Document 802.15-04-0137r4*, 2005.

[3] Z. N. Chen, T. S. P. See, and X. Qing, "Small printed ultrawideband antenna with reduced ground plane effect," *IEEE Trans. Antennas. Propag.*, vol. 55, no. 2, pp. 383–388, Feb. 2007.

[4] J. R. Verbiest and G. A. E. Vandenbosch, "A novel small-size printed tapered monopole antenna for UWB WBAN," *IEEE Antennas Wireless Propag. Lett.*, vol. 5, pp. 377–379, 2006.

[5] S. Radiom, H. Aliakbarian, G. A. E. Vandenbosch, and G. G. E. Gielen, "An effective technique for symmetric planar monopole antenna miniaturization," *IEEE Trans. Antennas. Propag.*, vol. 57, no. 10, pp. 2989–2996, Oct. 2009.

[6] D. Valderas, R. Alvarez, J. Melendez, I. Gurutzeaga, J. Legarda, and J. I. Sancho, "UWB staircase-profile printed monopole design," *IEEE Antennas Wireless Propag. Lett.*, vol. 7, pp. 255–259, 2008.

[7] M. Gopikrishna, D. D. Krishna, C. K. Anandan, P. Mohanan, and K. Vasudevan, "Design of a compact semi-elliptic monopole slot antenna for UWB systems," *IEEE Trans. Antennas. Propag.*, vol. 57, no. 6, pp. 1834–1837, Jun. 2009.

[8] A. M. Abbosh and M. E. Bialkowski, "Design of ultrawideband planar monopole antennas of circular and elliptical shape," *IEEE Trans. Antennas. Propag.*, vol. 56, no. 1, pp. 17–23, Jan. 2008.

[9] T. Dissanayake and K. P. Esselle, "UWB performance of compact L-shaped wide slot antennas," *IEEE Trans. Antennas. Propag.*, vol. 56, no. 4, pp. 1183–1187, Apr. 2008.

[10] K. S. Ryu and A. A. Kishk, "UWB antenna with single or dual band-notches for lower WLAN band and upper WLAN band," *IEEE Trans. Antennas. Propag.*, vol. 57, no. 12, pp. 3942–3950, Dec. 2009.

[11] R. Zaker, C. Ghobadi, and J. Nourinia, "Bandwidth enhancement of novel compact single and dual band-notched printed monopole antenna with a pair of L-shaped slots," *IEEE Trans. Antennas. Propag.*, vol. 57, no. 12, pp. 3978–3983, Dec. 2009.

[12] Q.-X. Chu and L.-H. Ye, "Design of compact dual-wideband antenna with assembled monopoles," *IEEE Trans. Antennas. Propag.*, vol. 58, no. 12, pp. 4063–4066, Dec. 2010.

[13] B. S. Yildirim, B. A. Cetiner, G. Roquetra, and L. Jofre, "Integrated bluetooth and UWB antenna," *IEEE Antennas Wireless Propag. Lett.*, vol. 8, pp. 149–152, 2009.

[14] R. K. Gupta, "Printed tri-band monopole antenna structures for wireless applications," *Microw. Opt. Technol. Lett.*, vol. 51, no. 7, pp. 1781–1785, Jul. 2009.

[15] W. Li, L. Cai, B. You, and C. Huang, "Design of printed notched-monopole UWB antenna," in *Proc. IEEE Int. Conf on Intelligent Computing and Intelligent Systems*, 2009, vol. 3, pp. 271–274.

[16] S. Mohammad Ali Nezhad and H. R. Hassani, "A novel tri-band E-shaped printed monopole antenna for MIMO application," *IEEE Antennas Wireless Propag. Lett.*, vol. 9, pp. 576–579, 2010.

[17] A. Vasylchenko, Y. Schols, W. De Raedt, and G. A. E. Vandenbosch, "Quality assessment of computational techniques and software tools for planar-antenna analysis," *IEEE Antennas Propag. Mag.*, vol. 51, no. 1, pp. 23–38, Feb. 2009.

[18] J. X. Xiao, M. F. Wang, and G. J. Li, "A ring monopole antenna for UWB application," *Microw. Opt. Technol. Lett.*, vol. 52, no. 1, pp. 179–182, Jan. 2010.

[19] K. Bahadori and Y. Rahmat-Samii, "A miniaturized elliptic-card UWB antenna with WLAN band rejection for wireless communications," *IEEE Trans. Antennas. Propag.*, vol. 55, no. 11, pp. 3326–3332, Nov. 2007.

Wideband Omnidirectional Circularly Polarized Dielectric Resonator Antenna With Parasitic Strips

Y. M. Pan and K. W. Leung

***Abstract*—A wideband omnidirectional circularly polarized (CP) rectangular dielectric resonator antenna (DRA) is investigated in this communication. An inclined slot, loaded by a parasitic conducting strip, is fabricated on each sidewall of the DRA. The parasitic strips can excite a CP mode, which combines with the CP DRA mode to provide a wideband axial-ratio (AR) bandwidth of more than 25%. To fully utilize the increased AR bandwidth, the impedance bandwidth is also broadened by introducing a hollow cylinder at the center of the DRA. The hollow region is also used to accommodate a coaxial probe that excites the antenna. The reflection coefficient, AR, radiation pattern, antenna gain, and efficiency of the antenna are studied, and reasonable agreement between the measured and simulated results is observed. A parametric study was also carried out to characterize the proposed wideband CP omnidirectional antenna.**

***Index Terms*—Circular polarization, dielectric resonator antenna (DRA), omnidirectional antenna, parasitic strips, wideband antenna.**

I. INTRODUCTION

Due to a number of attractive features such as its small size, low loss, wide bandwidth, and ease of excitation, the dielectric resonator antenna (DRA) has been studied extensively in the past two decades [1], [2]. Various antenna geometries, excitation schemes, and bandwidth enhancement techniques for designs of DRA have been developed. Thus far, studies of the DRA have mainly focused on broadside radiation modes [3]–[5], and relatively much less attention has been paid on omnidirectional radiation modes [6]–[10]. However, the omnidirectional circularly polarized (CP) antenna is very attractive in wireless communications because it can alleviate the multipath problem caused by reflections from building walls and the ground surface. Also, it can help stabilize the signal transmission and provide larger signal coverage [11]. Conventional omnidirectional CP designs were usually realized by using patch [11], [12] slot [13] and dipole antennas [14]. Recently, an omnidirectional rectangular DRA excited in its fundamental TM mode was investigated [15]. When a rectangular DRA is centrally fed by a coaxial probe, it will generate linearly polarized (LP) fields with the radiation pattern similar to that of a short electric monopole.

Manuscript received August 23, 2011; revised November 14, 2011; accepted December 22, 2011. Date of publication April 13, 2012; date of current version May 29, 2012. This work was supported by a GRF grant from the Research Grants Council of Hong Kong Special Administrative Region, China (Project No.: 116911).

The authors are with the State Key Laboratory of Millimeter Waves and Department of Electronic Engineering, City University of Hong Kong, Hong Kong SAR (e-mail: yongmpan@cityu.edu.hk; eekleung@cityu.edu.hk).

Color versions of one or more of the figures in this communication are available online at http://ieeexplore.ieee.org.

Digital Object Identifier 10.1109/TAP.2012.2194678